New Phytologist Supporting Information

Nutrient cycling drives plant community trait assembly and ecosystem functioning in a tropical mountain biodiversity hotspot

Authors: Mateus Dantas de Paula, Matthew Forrest, Liam Langan, Jörg Bendix, Jürgen Homeier, Andre Velescu, Wolfgang Wilcke, Thomas Hickler.

Article acceptance date: 28 June 2021

Notes S1 Competition and selection mechanisms of LPJ-GUESS and LPJ-GUESS-NTD

As described the main manuscript, individuals are established with randomly drawn values of SLA and WSG from the uniform parameter-defined trait range. These trait values are fixed for their lifetimes and determine an individual's strategy and therefore how competitive it is. Filtering occurs as mortality of less competitive individuals. This process relies on the existing competition and mortality processes found in the standard version of LPJ-GUESS. Mortality in LPJ-GUESS can occur from several factors: max longevity, low growth efficiency, temperature stress, fire and recurring disturbances (Smith *et al.*, 2001), of which the most relevant in our LPJ-GUESS-NTD is growth efficiency mortality.

Growth efficiency is determined as the ratio of individual net annual production (NPP) to leaf area. Individual NPP is a direct function of photosynthesis, which is subject to limitation pending the availability to the key resources of water, light and nutrients. Since these resources are finite, NPP and related resource acquisition is central to the competition dynamics for two reasons. Firstly, plants need sufficiently high NPP to avoid growth efficiency mortality. Secondly, by acquiring resources more effectively, competitive individuals are denying them to their competitors. This in turn reduces the competitor's at NPP and puts it at risk of growth efficiency mortality. We will now describe in a little more detail exactly how the trait values affect competition.

The susceptibility of an individual to mortality due to low growth efficiency is determined by its WSG, with lower WSG individuals more susceptible to dying from lower growth efficiency, as described by (Sakschewski *et al.*, 2015). This creates a competitive trade-off in that model that while low-WSG trees can increase in size with less carbon and shade high-WSG trees, they are also more susceptible to growth-efficiency mortality during their lifetimes.

An individual's SLA value influences its resource acquisition and demand. High SLA individuals have larger leaf areas per carbon investment which allows them to capture more light than low SLA individuals. However they also have higher nutritional (N and P) demands, (which defined at establishment through SLA tradeoffs, see section 1.2). When the individual is not able to meet N or P demands through nutrient update, its photosynthesis becomes limited, resulting in less NPP being available for growth and an increased risk of growth efficiency mortality. In contrast, low SLA individuals become less photosynthesis-limited in low nutrient environments due to their lower nutritional demands, and so would be able maintain higher photosynthetic rates in such environments.

Furthermore, a stressed individual in LPJ-GUESS-NTD responds by increasing its allocation of NPP to root growth, at the cost of allocation of leaves, as well as increasing nutrient reabsorption before leaf shedding. Increased root allocation increases root biomass and area, also nutrient uptake which may alleviate stress (see Notes S2 section 2.3). It should be pointed out that an individual's ability to do this does not depend on its randomly determined trait values, all individuals will respond to nutrient limitation by increasing root allocation. The emergent community trait distribution and ecosystem processes is finally a result of all these interacting factors, together with environmental drivers such as temperature, precipitation, nutrient deposition and soil.

Notes S2 Further modifications of LPJ-GUESS

2.1 Vegetation processes

Plant growth in LPJ-GUESS is restricted by temperature responses of photosynthesis and respiration, and PFT establishment and survival is also constrained by bioclimatic limits. This allows the separation of temperate and tropical PFTs, for example. This approach introduces an abrupt PFT shift along the elevational gradient whereas real trait changes are rather continuous. Therefore, we harmonized the photosynthesis-temperature-response of tropical and temperature tree species in the original LPJ-GUESS with two modifications. First, we merge the photosynthesis response parameters to temperature in C_3 plants in tropical and temperate species. This was done by setting the lower bounds of temperature response to the temperate parameters, and the upper bound to tropical parameters. Typically, photosynthesis functions without harm between 0 and 30ºC, which can shift from a range of 7 – 40ºC to 15 – 45ºC for extreme environment specialists (Sage & Kubien, 2007). We do not expect therefore the photosynthesis to be affected by temperature within the average monthly temperature ranges of the elevation gradient (10 - 20ºC). Second, respiration acclimation was changed from a fixed calibrated parameter (1.0 for temperate species, 0.15 for tropical species) to a temperature dependent factor, which was developed for the QUINCY model (Atkin *et al.*, 2014; Thum *et al.*, 2019). This provides a more mechanistic approach to respiration temperature acclimation.

Photosynthesis and the associated canopy fluxes are calculated using a scheme based on the approach of BIOME3 (Haxeltine & Prentice, 1996) which uses the “big-leaf” approximation (Luo *et al.*, 2018) to integrate across the leaves of plant individuals with different leaf traits. Thus, vegetation dynamics and competition for resources are more detailed than in traditional models but not the integration of canopy fluxes at the stand level.

The light intercepted by each individual is calculated daily using the Lambert-Beer law and incoming light available is reduced according to the light previously intercepted by taller individuals (Smith *et al.*, 2001). It should be noted that LPJ-GUESS is not spatially explicit (individuals do not have specific x-y positions) so the formulation is a one dimensional "box model" where all individuals compete with all the other individuals. Individuals which acquire lower fractions of the available light face higher growth efficiency mortality rates due to their resultant lower NPP, which will particularly effect for those with lower wood specific gravity (WSG) values. This defines an implicit trade-off in the model: individuals with lower WSG can grow taller (for the same carbon investment into wood) but suffer a higher risk of growth efficiency mortality should they become shaded by taller individuals.

2.2 Trait tradeoffs

Below we describe how trait trade-offs are used to calculate trait values from the randomly selected SLA and WSG values.

- Tissue stoichiometry and photosynthesis: In LPJ-GUESS, tissue (leaf, root and sapwood) C:N ratios are defined by model parameters for each plant functional type, and determine plant N demand and tissue N concentration (Smith *et al.*, 2014). Leaf N concentration in turn determines the maximum photosynthetic capacity and, through litterfall, also influences soil carbon and nitrogen dynamics, which are based on the CENTURY model (Smith *et al.*, 2014). In the model version here, optimal leaf C:N ratios are derived from the randomized SLA values defined at establishment, using correlations from the local field measurements (Fig. S1a), an improvement in relation to global relationships estimated from the TRY (Kattge *et al.*, 2020) database (Fig. S1b). In the standard LPJ-GUESS model, realized leaf C:N ratios (i.e. leaf C:N after N uptake) vary by up to ±89% in relation to optimal values in response to N uptake. This implementation was based on the range of leaf C:N values observed for all tree species in a temperate broadleaf forest, as measured by White et al. (2000). Based on our field data (Báez & Homeier, 2018), we reduced the potential variation to ±24%. As in the standard LPJ-GUESS model, it was assumed that sapwood and fine root N concentrations vary in tandem with the leaf N concentration (with C:N ratios of sapwood being approximately seven times higher than in leaves; (Friend *et al.*, 1997)).

The same approach has been adopted to add tissue P concentrations to the model. As for C:N ratios, optimal tissue C:P ratios are defined, from establishment for each individual by a correlation with the randomized SLA, using field measured leaf C:P data from the same dataset (Fig. S1c). Fine root and sapwood P, as well as intra-PFT variation of C:P, long-term P storage and P retranslocation are simulated as for N in (Smith *et al.*, 2014). However, the response of photosynthesis to leaf P concentrations is calculated using a separate function, relating leaf P to carbon assimilation rates. For this, the relationship for C_3 plants by Ghannoum et al. (2008) was used. The photosynthesis response of leaves to the active leaf P concentration is defined by:

Eq. S1 $$A_{max} = 6.6 + 10.1 \cdot P$$

Where Amax is the maximum assimilation rate in µmol m^{-2} s^{-1}, and P is in mmol m^{-2}.

- Leaf longevity: According to the leaf economic spectrum, SLA is negatively related to leaf longevity (Wright *et al.*, 2004) and therefore influences the rate of litterfall (leaf turnover). For this tradeoff only community-averaged values for each elevation were available, therefore the relationship was calculated from the TRY database for woody angiosperms (Kattge *et al.*, 2020). The average observation data for five single plots (Moser *et al.*, 2007) fell in the confidence range of the regression function derived from TRY (Fig. S1d). Fine root longevity or turnover was kept fixed at standard model values (0.7 per year), and not related to tissue stoichiometry, since trends along the altitudinal gradient do not show a clear pattern (Graefe *et al.*, 2008).

- Growth efficiency mortality (i.e. mortality rate as a function of NPP per leaf area) as a function of WSG: The representation of mortality in dynamic global vegetation and Earth System Models has been long considered a challenge because of lack of data (Sakschewski *et al.*, 2016). We adopted the negative correlation of growth efficiency mortality with wood density by (King *et al.*, 2006), which was also used in LPJmL-FIT (Sakschewski *et al.*, 2015).

2.3 Changes to plasticity traits: leaf to shoot ratio and nutrient resorption

In addition to limitations in carbon assimilation rates because of lower-than-optimal N or P concentrations, photosynthesis may also be limited in the model by temperature, soil water content and radiation. Water, N and P demand (which varies according to the individual´s trait combination) may limit growth in response to environmental conditions and drive cumulative changes in plant traits (plasticity traits) (de Kroon, 2010). In this study, we allow cumulative changes from an initial average value for two key individual traits, leaf to fine root ratio of carbon allocation (LTOR) and nutrient (N and P) resorption (Fig. 1). In the original LPJ-GUESS

model, LTOR is allowed to vary according to water or nutrient stress (defined as realized nutrient content of tissue after uptake divided by optimal values of tissue nutrient content for that trait combination). Increased allocation to fine roots (i.e. lower LTOR values), aims to represent a plant strategy to alleviate stress, since in the model root surface area for uptake is dependent on fine root biomass. In LPJ-GUESS, LTOR was fixed for tree PFT at a maximum of 1.0 (equal C allocation to leaves and fine roots) and allowed to be reduced according to N stress (defined as difference between optimal and realized leaf N concentration) or water stress. However, along the elevation gradient, this allocation can vary on average between 1.6 and 0.5 (Table S2), from 1,000 m (less nutrient stressed) to 3,000 m a.s.l. (more nutrient stressed), meaning that the trees may allocate more than double the amount of carbon to leaves in the less stressed site, or the same proportion to fine roots in the more stressed site. In LPJ-GUESS-NTD, each individual from establishment starts with a LTOR value of 1.0 (standard LPJ-GUESS value), and according to water stress or the difference of optimal and realized N or P leaf content, is allowed to increase or decrease leaf or fine root mass allocation yearly and cumulatively as shown in Eqs. S2-4:

Eq. S2
$$\frac{d\,LTOR_t}{dt} = min\left(d\,S_N, dS_P\right) \cdot LTOR_{t-1}$$

with,

Eq. S3
$$\frac{dS_N}{dt} = \frac{C:N_t}{C:N_{opt}}$$

Eq. S4
$$\frac{dS_P}{dt} = \frac{C:P_t}{C:P_{opt}}$$

where S_N and S_P are the N or P stress levels for the yearly timestep t, $C{:}N_t$ and $C{:}P_t$ are the realized C to N or P ratios after nutrient uptake and $C{:}N_{opt}$ and $C{:}P_{opt}$ are the optimal C to N/P ratios defined by using the local tradeoff relationships. This approach includes the possibility of more C allocated to leaves than roots proportionally. This reproduces a gradual change of the leaf to fine root biomass ratio into adulthood towards an allometry in which the individual tree no longer faces stress (or as far as nutrient or water competition in the environment allows). Due

to the cumulative nature of the LPJ-GUESS-NTD allocation, a wider range of LTOR values can be reached, with important implications for future sudden environmental change scenarios, which may affect disproportionally trees grown in low stressed conditions.

Before shedding their leaves, plants reabsorb part of the nutrients according to their current stress levels (Vergutz *et al.*, 2012). Although this value was fixed at 50% in LPJ-GUESS, field measurements indicate that trees reabsorb on average 20 – 55% of their nutrients from low to higher stressed environments along the elevation gradient (Wolf *et al.*, 2011). In our model, nutrient resorption of N (*rN*) and P (*rP*) was allowed to vary independently and cumulatively from a starting establishment value of 0.5 (standard LPJ-GUESS value) to any value between 0 and 1.0 (Eq. S5).

Eq. S5
$$\frac{d\,rN_t, rP_t}{dt} = min\left(d\,S_N, dS_P\right) \cdot rN_{t-1}, rP_{t-1}$$

2.4 Equations and parameters used for the P cycle

Parameters and equations from Wang *et al.*, (2010) were: Phosphorus saturation values for the soil organic matter with a minimum N:P concentration ratio of 4; Sorption of phosphorus was driven by the Eqs S6-S8:

Eq. S6
$$\frac{d\,P_{sorb}}{dt} = \frac{k_{plab} \cdot Sp_{max}}{\left(k_{plab} + P_{lab}\right)^2} \cdot \frac{d\,P_{lab}}{dt}$$

Eq. S7
$$\frac{d\,P_{ssb}}{dt} = \mu_{sorb} \cdot P_{sorb} - \mu_{ssb} \cdot P_{ssb}$$

Eq. S8
$$P_{cc} = v_{sc} \cdot P_{ssb}$$

Where P_{sorb} is the sorbed phosphorus pool, P_{ssb} is the strongly sorbed phosphorus pool, P_{cc} is the occluded phosphorus pool, u_{sorb} and u_{ssorb} are 0.0067 year^{-1}, s_{Pmax} and k_{Plab} are soil specific (Entisol for the simulated site) maximum amount of sorbed P (0.064) and constant for adsorption of P

(0.050) respectively (both in P kg m^{-2}), and vsc is the rate of transfer to the occluded pool from the strongly sorbed pool (10^{-5} $year^{-1}$).

Notes S3 Soil sampling and chemical analyses

We excavated three soil profiles on each plot to 1 m mineral soil depth or until reaching the parent material and collected disturbed and undisturbed samples from each horizon. At all soil profiles we measured bulk density of the soil horizons with undisturbed cores (100 cm^3). We determined ammonium (NH_4-N) and nitrate (NO_3-N) concentrations in the mineral soil using field-fresh material, immediately after sample collection in Ecuador. Both mineral nitrogen species were extracted with 1 M KCl in the laboratory of the research station San Francisco, frozen to -20 °C and transported in frozen state to Germany for chemical analyses by continuous flow analysis (CFA) using high resolution colorimetry and photometric detection (Skalar, San++, Breda, Germany). During the CFA measurements, samples were dialyzed on-line and NH_4-N was determined by the Berthelot reaction. Ammonia is buffered and chlorinated to monochloramine which reacts with salicylate to 5-aminosalicylate. After oxidation and oxidative coupling, a green coloured complex is formed, which is measured at 660 nm. For NO_3-N determination, the sample is buffered at pH 8.2, dialyzed on-line, and passed through a column containing granulated copper-cadmium to reduce the nitrate to nitrite, which is determined by diazotizing with sulfanilamide and coupling with N-(1-naphthyl) ethylenediamine dihydrochloride to form a highly coloured azo dye which is measured at 540 nm. The determination of NO_3-N concentrations by cadmium reduction usually includes a small amount of originally present nitrite-N (NO_2-N), which was below the detection limits and hence considered negligible. We calculated NH_4-N and NO_3-N stocks in the mineral soil (0-0.3 m) from the horizon-specific data (bulk density, horizon thickness and water content corrected concentrations in each soil horizon).

Table S1. New parameters implemented into LPJ-GUESS-NTD. All other parameters are unchanged from LPJ-GUESS version 4.0 (Smith *et al.*, 2014)

Variable	Description	Unit	Value(s)	Reference
sla_min	minimum randomized specific leaf area	$cm^2\ g^{-1}$	15.5	(Báez & Homeier, 2018)
sla_max	maximum randomized specific leaf area	$cm^2\ g^{-1}$	273.5	(Báez & Homeier, 2018)
sla_range	number of possible random values (trait resolution)	-	300	this study
sla_avg	average gradient SLA across elevation gradient (value for low diversity (LD) scenario)	$cm^2\ g^{-1}$	82.5	this study
wsg_min	minimum randomized wood specific gravity	$g\ cm^{-3}$	0.158	(Báez & Homeier, 2018)
wsg_max	maximum randomized wood specific gravity	$g\ cm^{-3}$	1.02	(Báez & Homeier, 2018)
wsg_range	number of possible random values (trait resolution)	-	300	this study
wsg_avg	average gradient wsg (value for low diversity (LD) scenario)	$g\ cm^{-3}$	0.563	this study
frac_mintomax	fraction between min and max C:N and C:P values due to stress	-	1.48 (±24% to average)	(Báez & Homeier, 2018)
Michaelis-Menten kinetics				
nuptoroot	Max. NH_4 mass uptake per fine root C mass per day	$gN\ gC^{-1}\ d^{-1}$	$8.9\ 10^{-3}$	(Rothstein *et al.*, 2000)
puptoroot	Max. PO_4 mass uptake per fine root C mass per day	$gP\ gC^{-1}\ d^{-1}$	$2.5\ 10^{-3}$	(Kavka & Polle, 2016)
KmN_volume	Half saturation concentration for NH_4 uptake	$kg\ l^{-1}$	$2.03\ 10^{-6}$	(Rothstein *et al.*, 2000)
KmP_volume	Half saturation concentration for PO_4 uptake	$kg\ l^{-1}$	5 10-8	(Mulder & Hendriks, 2014)
Non - Michaelis-Menten kinectics				
no3uptoroot	Max. NO3- mass uptake per fine root C mass per day	$gNO_3.gC^{-1}\ d^{-1}$	0.05	(Rothstein *et al.*, 2000)

Table S2. Reference values taken from field and laboratory measurements at the three study sites at 1000 m a.s.l. (Bombuscaro), 2000 m a.s.l. (Reserva Biológica San Francisco) and 3000 m a.s.l. (Cajanuma) used to parametrize and evaluate the model.

Elevation (m a.s.l.)									
Variable	**Unit**	**Data type**	**1000**		**2000**		**3000**		**Ref.**
			Mean	**CI**	**Mean**	**CI**	**Mean**	**CI**	
Temperature	°C	Input	20.20	0.24	15.20	0.33	9.90	0.36	(Peters & Richter, 2009; Rollenbeck *et al.*, 2015; Bendix *et al.*, 2018; Dobbermann *et al.*, 2018; Bendix, 2020)
Precipitation	mm $month^{-1}$	Input	152.00	22.46	151.00	26.31	182.00	43.51	(Peters & Richter, 2009; Rollenbeck *et al.*, 2015; Bendix *et al.*, 2018; Dobbermann *et al.*, 2018; Bendix, 2020)
Radiation	W m^{-2}	Input	164.90	25.40	155.50	11.66	153.70	22.35	(Peters & Richter, 2009; Rollenbeck *et al.*, 2015; Bendix *et al.*, 2018; Dobbermann *et al.*, 2018; Bendix, 2020)
NH_4-N + NO_3-N soil input (Stemflow + Throughfall)	kg ha^{-1} y^{-1}	Input			19.07	2.02			(Wilcke *et al.*, 2013; Velescu *et al.*, 2020a; Velescu & Wilcke, 2020a,b)
PO_4 soil input (Stemflow + Throughfall)	kg ha^{-1} y^{-1}	Input			3.31	0.40			(Wilcke *et al.*, 2019; Velescu *et al.*, 2020a; Velescu & Wilcke, 2020a,b)

Specific Leaf Area	$cm^2\ g^{-1}$	Evaluation	104.30	6.00	82.50	5.08	53.90	3.87	(Homeier, 2017a,b; Báez & Homeier, 2018)
Wood Specific Gravity	$g\ cm^{-3}$	Evaluation	0.56	0.02	0.53	0.01	0.61	0.01	(Homeier, 2017a,b; Báez & Homeier, 2018)
Leaf C:N ratio	-	Evaluation	26.10	1.00	29.10	1.42	42.90	1.93	(Homeier, 2017a,b; Báez & Homeier, 2018)
Leaf C:P ratio	-	Evaluation	748.10	49.05	677.70	44.16	1125.6	77.92	(Homeier, 2017a,b; Báez & Homeier, 2018)
Leaf Turnover	y^{-1}	Evaluation	0.74		0.51		0.49		(Moser *et al.*, 2007)
Nitrogen Use Efficiency	-	Evaluation	62.90	2.69	55.20	15.14	103.10	33.34	(Wolf *et al.*, 2011)
Phosphorus Use Efficiency	-	Evaluation	1298.70	116.66	1075.3	566.54	2325	942.99	(Wolf *et al.*, 2011)
Above+Below ground Carbon	$Mg\ ha^{-1}$	Evaluation	109.00	17.64	104.00	25.48	60.00	7.84	(Leuschner *et al.*, 2013)
NPP	$Mg\ ha^{-1}\ y^{-1}$	Evaluation	8.59	0.81	8.93	1.08	4.33	0.35	(Wallis *et al.*, 2019)
Leaf:Fine Root ratio (C basis)	-	Evaluation	1.61		1.21		0.44		(Leuschner *et al.*, 2013)
Litter N deposition	$kg\ ha^{-1}\ y^{-1}$	Evaluation	58.36	11.00	81.26	31.79	22.65	7.002	(Wolf *et al.*, 2011)

Litter P deposition	kg ha^{-1} y^{-1}	Evaluation	2.83	0.68	4.73	2.55	1.02	0.42	(Wolf *et al.*, 2011)
Soil inorganic Ni (NH_4-N + NO_3-N)	kg ha^{-1}	Evaluation	5.16	4.29	13.02	6.59	1.95	0.64	This study, (Velescu *et al.*, 2020b,c,d)

Table S3. Summary statistics of the simulated and observed trait distributions

Site (m)	Type	Mean	Variance	SD	Median	First quartile	Third Quartile	IQR
SLA ($cm^2 g^{-1}$)								
1,000	NTD	119.34	4305.07	65.61	106	64.5	167	102.5
	Nlim-OFF	212.7	1853.22	43.05	219.5	183	248.5	65.5
	Field	104.4	1357.69	36.85	100.7	77.83	121.32	43.49
2,000	NTD	85.53	3320.84	57.63	67	43	114.5	71.5
	Nlim-OFF	210.47	2126.61	46.12	219.5	180	248.5	68.5
	Field	82.58	1689.30	41.1	72.8	53.7	95	41.3
3,000	NTD	36.31	639.33	25.29	31	23	41.5	18.5
	Nlim-OFF	210.33	1988.27	44.59	218.5	180.5	247	66.5
	Field	53.88	577.00	24.02	48.58	37.35	65.77	28.42
WSG ($g\ cm^{-3}$)								
1,000	NTD	0.6312	0.1900	0.1947	0.6178	0.4798	0.7786	0.2988
	Nlim-OFF	0.2683	0.0900	0.0894	0.2500	0.2010	0.3046	0.1036
	Field	0.5592	0.1400	0.1386	0.5400	0.4500	0.6600	0.2100
2,000	NTD	0.6672	0.2100	0.2079	0.6780	0.5028	0.8418	0.3390
	Nlim-OFF	0.2673	0.1000	0.1044	0.2328	0.1924	0.2988	0.1064
	Field	0.5271	0.1200	0.1239	0.5200	0.4400	0.6200	0.1800
3,000	NTD	0.6869	0.2100	0.2099	0.7010	0.5230	0.8678	0.3448
	Nlim-OFF	0.3340	0.1400	0.1374	0.3074	0.2270	0.4108	0.1838
	Field	0.6050	0.0800	0.0825	0.6000	0.5600	0.6500	0.0900

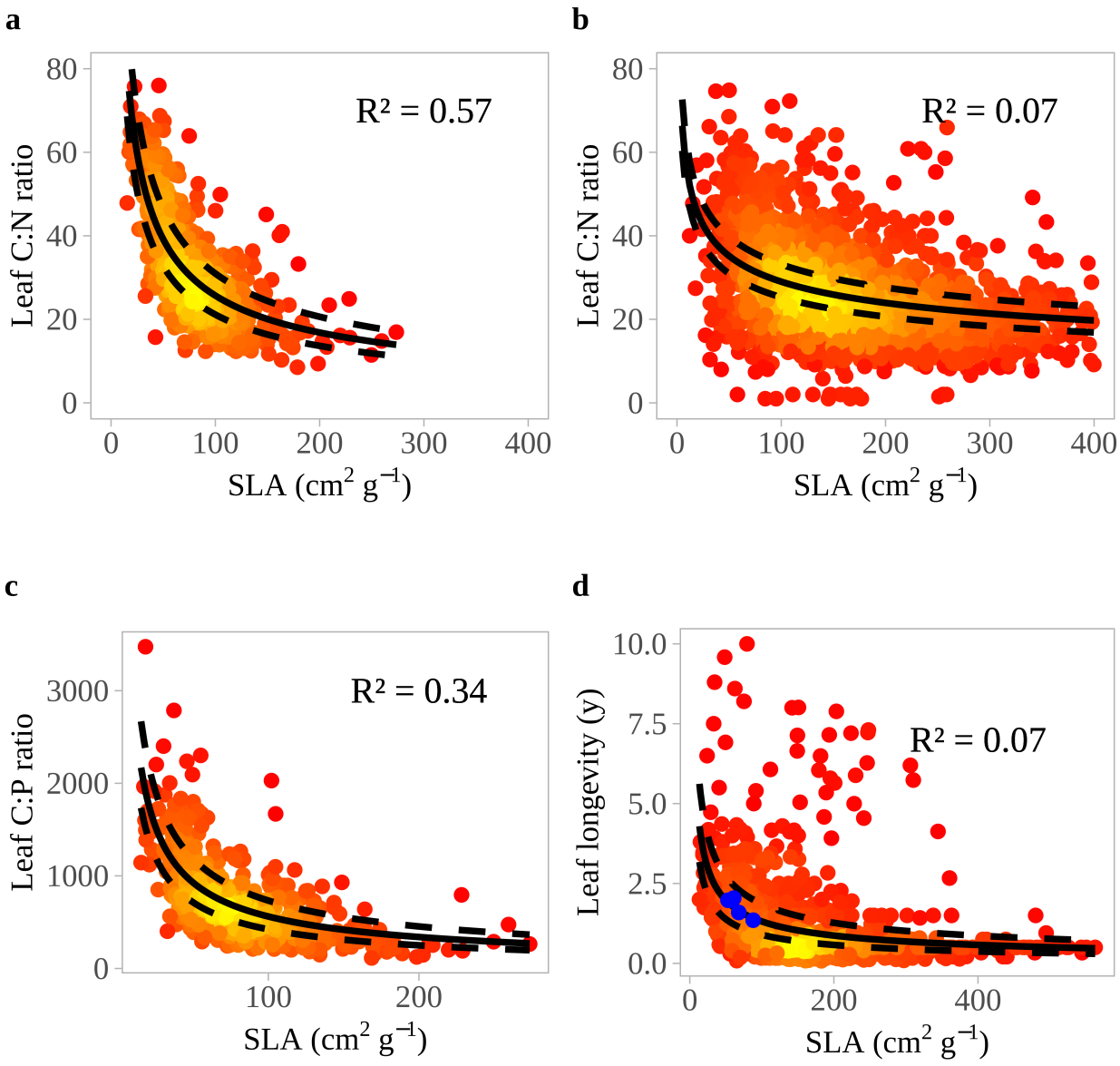

Figure S1. Trait-trait relationships used in the LPJ-GUESS-NTD trait variability module, fitted using power laws. SLA: Specific Leaf Area. C:N and C:P ratios are mass-based. The relationships shown in the left column (a, c) were produced using local species data from Báez & Homeier (2018), the relationships in the right column (b, d) were taken from the TRY database for all angiosperms (Kattge *et al.*, 2020). Blue points in the lower right panel represent site averages (1000, 1050, 2000, 2050, 3000 m a.s.l.) measured at 2000 m a.s.l. by Moser *et al.* (2007). Dotted black lines represent standard errors.

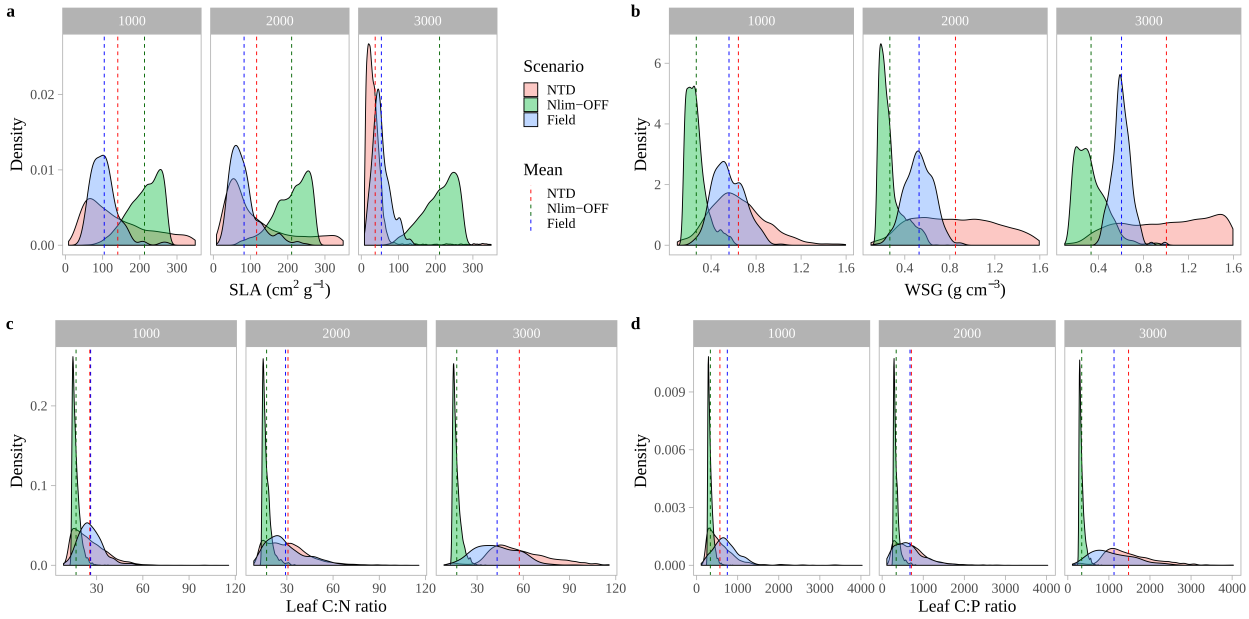

Figure S2. Expanded trait range (min - max: SLA = 5.0 - 350.0 $cm^2\ g^{-1}$; WSG = 0.1 - 1.6 $g\ cm^{-3}$) simulated and observed community trait frequencies for (a) specific leaf area (SLA), (b) wood specific gravity (WSG), (c) Carbon to nitrogen (C:N) and (d) carbon to phosphorus (C:P) concentration ratios in leaves ratios along the elevational gradient (1,000, 2,000 and 3,000 m a.s.l.). Scenarios refer to the Nutrient-Trait-Dynamics mode (NTD); nutrient limitation off, trait variation on (Nlim-OFF) and field observations.

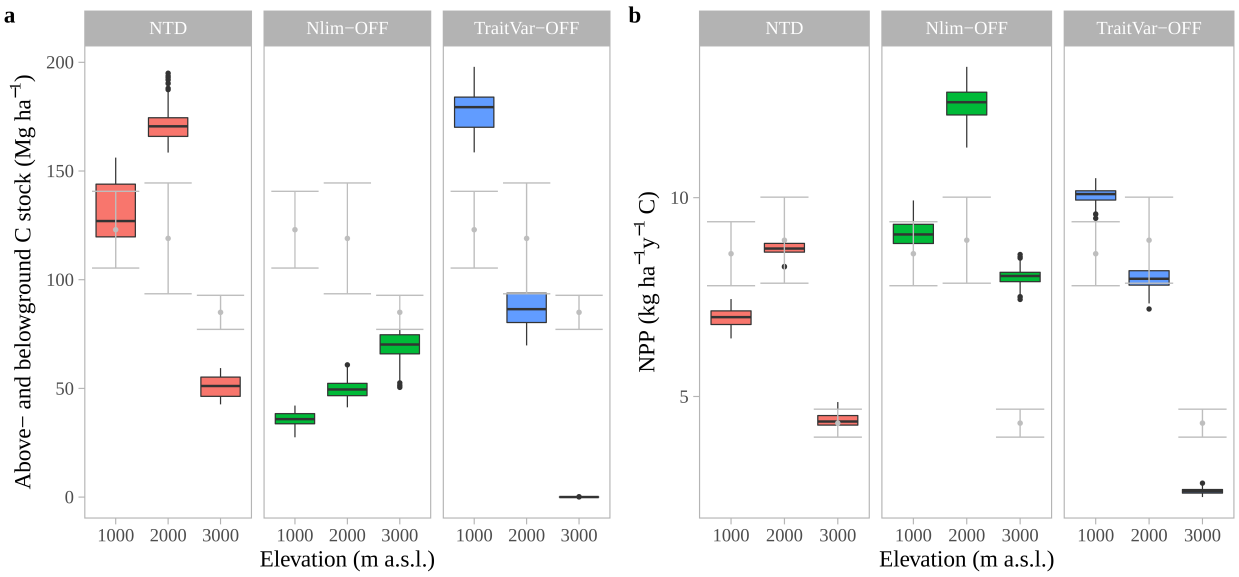

Figure S3. Expanded trait range (min - max: SLA = 5.0 - 350.0 $cm^2\ g^{-1}$; WSG = 0.1 - 1.6 $g\ cm^{-3}$) results for processes related to C along the elevational gradient (a) Above and belowground stocks and (b) Net Primary Production (NPP). Grey lines indicate means and confidence intervals for observations (N = 18 for each site) from field data (Leuschner et al., 2013). Scenarios refer to the Nutrient-Trait-Dynamics mode (NTD), nutrient limitation off, trait variation on (Nlim-OFF) and nutrient limitation on, trait variation off (TraitVar-OFF).

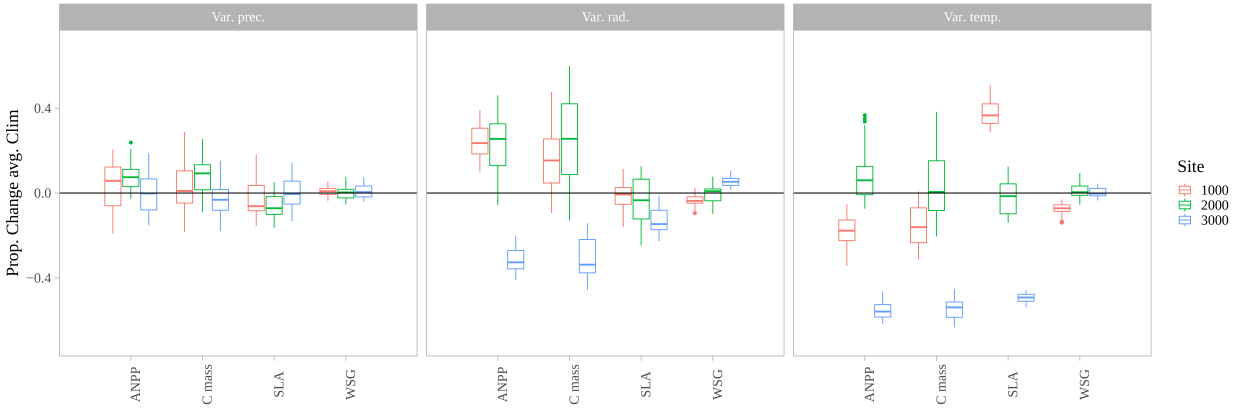

Figure S4. Climatic sensitivity analysis varying in turn temperature (Var. temp.), precipitation (Var. prec.) and radiation (Var. rad.) long the elevational gradient. Values refer to proportional changes in relation to a reference simulation in which all three drivers are set to average values.

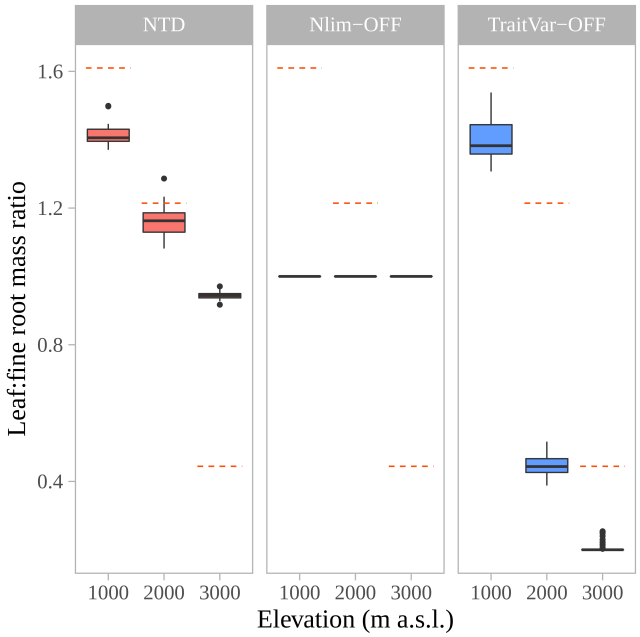

Figure S5. Modeled results of the leaf to fine root biomass ratio along the environmental gradient. Scenarios refer to the Nutrient-Trait-Dynamics mode (NTD), nutrient limitation off, trait variation on (Nlim-OFF) and nutrient limitation on, trait variation off (TraitVar-OFF). Dotted red lines are means from observations (Table S2).

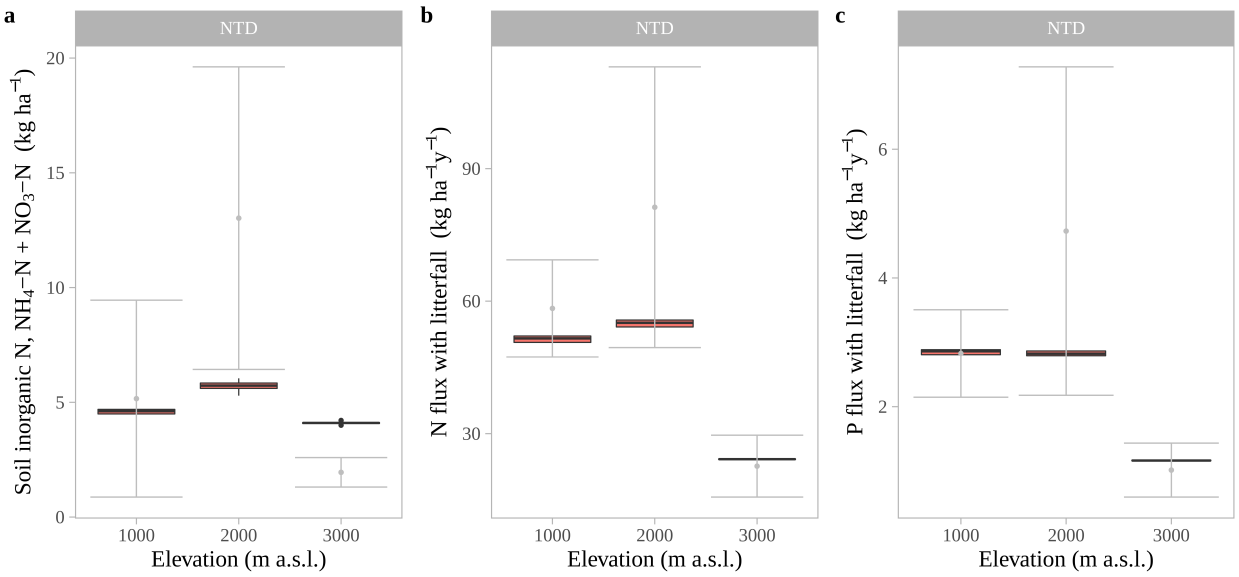

Figure S6. Simulation results of the 1 M KCl-extractable soil inorganic N stocks (NO_3-N + NH_4-N) in the Oi, Oe and Oa horizons (a) and litter nutrient returns of N (b) and P (c) along the elevation gradient. Grey lines indicate means and confidence intervals from field data (references in Table S2).

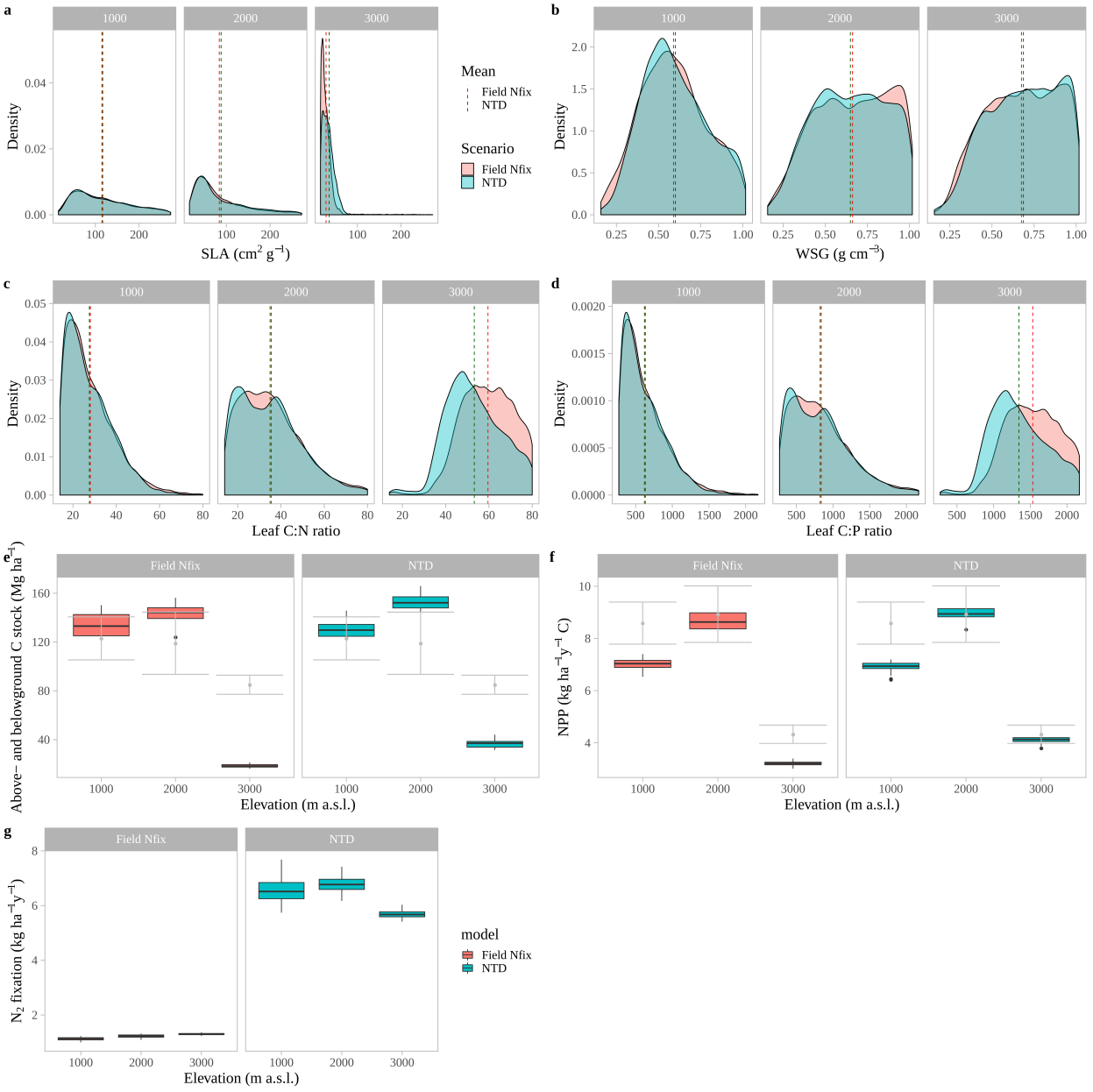

Figure S7. Simulated trait distributions comparing the effect of standard LPJ-GUESS N-fixing approach based on evapotranspiration and the prescribed N-fixation from field measurements (Field Nfix, max. 1.5 kg ha^{-1} y^{-1} N). (a) – (d): Comparison of trait distributions; (e) – (f): biomass and productivity; (g): N fixation.

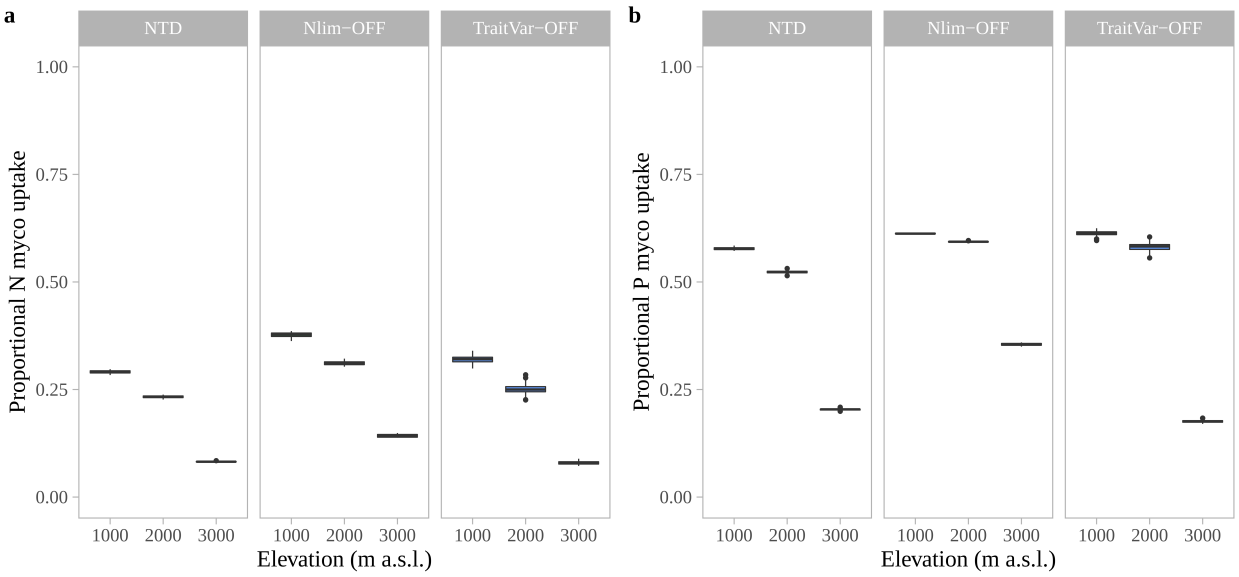

Figure S8. Proportional mycorrhizally-mediated plant (a) N and (b) P uptake in relation to direct plant nutrient uptake along the elevational gradient. Scenarios refer to Nutrient-Trait-Dynamics mode (NTD), nutrient limitation off, trait variation on (Nlim-OFF) and nutrient limitation on, trait variation off (TraitVar-OFF).

REFERENCES

Atkin OK, Meir P, Turnbull MH. **2014**. Improving representation of leaf respiration in large-scale predictive climate-vegetation models. *New Phytologist* **202**: 743–748.

Báez S, Homeier J. **2018**. Functional traits determine tree growth and ecosystem productivity of a tropical montane forest: Insights from a long-term nutrient manipulation experiment. *Global Change Biology* **24**: 399–409.

Bendix J. **2020**. Climate Station Data Cajanuma Paramo - daily estimate 1998 - 2018. *DFG-FOR816 Data Warehouse http://www.tropicalmountainforest.org/data_pre.do?citid=1858*.

Bendix J, Dobbermann M, Werner N. **2018**. Climate station data from ECSF Thies station 2018. *DFG-FOR816 Data Warehouse http://www.tropicalmountainforest.org/data_pre.do?citid=1713*.

Dobbermann M, Bendix J, Werner N. **2018**. Climate station data from Bombuscaro Thies station 2018. *DFG-FOR816 Data Warehouse http://www.tropicalmountainforest.org/data_pre.do?citid=1712*.

Friend AD, Stevens AK, Knox RG, Cannell MGR. **1997**. A process-based, terrestrial biosphere model of ecosystem dynamics (Hybrid v3.0). *Ecological Modelling* **95**: 249–287.

Ghannoum O, Paul MJ, Ward JL, Beale MH, Corol DI, Conroy JP. **2008**. The sensitivity of photosynthesis to phosphorus deficiency differs between C3 and C4 tropical grasses. *Functional Plant Biology* **35**: 213–221.

Graefe S, Hertel D, Leuschner C. **2008**. Estimating Fine Root Turnover in Tropical Forests along an Elevational Transect using Minirhizotrons. *Biotropica* **40**: 536–542.

Haxeltine A, Prentice TC. **1996**. BIOME3: An equilibrium terrestrial biosphere model based on ecophysiological constraints, resource availability, and competition among plant functional types. *Global Biogeochemical Cycles* **10**: 693–703.

Homeier J. **2017a**. Bombuscaro tree leaf and stem traits. *DFG-FOR816 Data Warehouse http://vhrz669.hrz.uni-marburg.de/tmf_respect/data_pre.do?citid=1648*.

Homeier J. **2017b**. Cajanuma tree leaf and stem traits. *DFG-FOR816 Data Warehouse http://vhrz669.hrz.uni-marburg.de/tmf_respect/data_pre.do?citid=1649*.

Kattge J, Bönisch G, Díaz S, Lavorel S, Prentice IC, Leadley P, Tautenhahn S, Werner GDA, Aakala T, Abedi M, *et al.* 2020. TRY plant trait database – enhanced coverage and open access. *Global Change Biology* **26**: 119–188.

Kavka M, Polle A. **2016**. Phosphate uptake kinetics and tissue-specific transporter expression profiles in poplar (Populus × canescens) at different phosphorus availabilities. *BMC Plant Biology* **16**: 1–14.

King DA, Davies SJ, Tan S, Noor NSM. **2006**. The role of wood density and stem support costs in the growth and mortality of tropical trees. *Journal of Ecology* **94**: 670–680.

de Kroon H. **2010**. Morphological Plasticity in Clonal Plants : The Foraging Concept Reconsidered Author (s): Hans de Kroons and Michael J . Hutchings Published by : British Ecological Society Stable URL : http://www.jstor.org/stable/2261158. *Society* **83**: 143–152.

Leuschner C, Zach A, Moser G, Soethe N, Graefe S, Hertel D, Iost S, Ro M, Horna V, Wolf K. **2013**. The Carbon Balance of Tropical Mountain Forests Along an Altitudinal Transect. In: Bendix J, ed. Ecosystem Services, Biodiversity and Environmental Change in a Tropical Mountain Ecosystem of South Ecuador. Springer-Verlag Berlin Heidelberg, 117–139.

Luo X, Chen JM, Liu J, Black TA, Croft H, Staebler R, He L, Arain MA, Chen B, Mo G, *et al.* 2018. Comparison of Big-Leaf, Two-Big-Leaf, and Two-Leaf Upscaling Schemes for Evapotranspiration Estimation Using Coupled Carbon-Water Modeling. *Journal of Geophysical Research: Biogeosciences* **123**: 207–225.

Moser G, Hertel D, Leuschner C, Moser G, Hertel D, Leuschner C. **2007**. Altitudinal Change in LAI and Stand Forests: a Transect Study in Ecuador Leaf Biomass in Tropical Montane and a Pan-Tropical Meta-Analysis. **10**: 924–935.

Mulder C, Hendriks AJ. **2014**. Half-saturation constants in functional responses. *Global Ecology and Conservation* **2**: 161–169.

Peters T, Richter M. **2009**. Climate Station Data at Bombuscaro. *DFG-FOR816 Data Warehouse http://www.tropicalmountainforest.org/data_pre.do?citid=501*.

Rollenbeck RT, Peters T, Emck P, Richter M. **2015**. ECSF Climate station best estimate Ver. 2. *DFG-FOR816 Data Warehouse http://www.tropicalmountainforest.org/data_pre.do?citid=1415*.

Rothstein DE, Zak DR, Pregitzer KS, Curtis PS. **2000**. Kinetics of nitrogen uptake by Populus tremuloides in relation to atmospheric CO2 and soil nitrogen availability. *Tree Physiology* **20**: 265–270.

Sage RF, Kubien DS. **2007**. The temperature response of C3 and C4 photosynthesis. *Plant, Cell and Environment* **30**: 1086–1106.

Sakschewski B, Von Bloh W, Boit A, Poorter L, Peña-Claros M, Heinke J, Joshi J, Thonicke K. **2016**. Resilience of Amazon forests emerges from plant trait diversity. *Nature Climate Change* **6**: 1032–1036.

Sakschewski B, von Bloh W, Boit A, Rammig A, Kattge J, Poorter L, Peñuelas J, Thonicke K. **2015**. Leaf and stem economics spectra drive diversity of functional plant traits in a dynamic global vegetation model. *Global Change Biology* **21**: 2711–2725.

Smith B, Prentice IC, Sykes MT. **2001**. Representation of vegetation dynamics in the modelling of terrestrial ecosystems: comparing two contrasting approaches within European climate space. *Global Ecology and Biogeography* **10**: 621–637.

Smith B, Wärlind D, Arneth A, Hickler T, Leadley P, Siltberg J, Zaehle S. **2014**. Implications of incorporating N cycling and N limitations on primary production in an individual-based dynamic vegetation model. *Biogeosciences* **11**: 2027–2054.

Thum T, Caldararu S, Engel J, Kern M, Pallandt M, Schnur R, Yu L, Zaehle S. **2019**. A new model of the coupled carbon, nitrogen, and phosphorus cycles in the terrestrial biosphere (QUINCY v1.0; revision 1996). *Geoscientific Model Development* **12**: 4781–4802.

Velescu A, Fabian T, Wilcke W. **2020a**. Water fluxes and element concentrations in throughfall in Bombuscaro between 2018-2019. *DFG-FOR816 Data Warehouse http://www.tropicalmountainforest.org/data_pre.do?citid=1863*.

Velescu A, Fabian T, Wilcke W. **2020b**. Chemical properties of forest and pasture soils in Bombuscaro at 1000 m asl. *DFG-FOR816 Data Warehouse http://www.tropicalmountainforest.org/data_pre.do?citid=1867*.

Velescu A, Fabian T, Wilcke W. **2020c**. Chemical properties of forest and pasture soils in San Francisco at 2000 m asl. *DFG-FOR816 Data Warehouse http://www.tropicalmountainforest.org/data_pre.do?citid=1868*.

Velescu A, Fabian T, Wilcke W. **2020d**. Chemical properties of forest and pasture soils in Cajanuma at 3000 m asl. *DFG-FOR816 Data Warehouse http://www.tropicalmountainforest.org/data_pre.do?citid=1869*.

Velescu A, Wilcke W. **2020a**. Water fluxes and element concentrations in throughfall in the microcatchment Q2 between 1998-2016. *DFG-FOR816 Data Warehouse http://www.tropicalmountainforest.org/data_pre.do?citid=1861*.

Velescu A, Wilcke W. **2020b**. Water fluxes and element concentrations in stem flow in the microcatchment Q2 between 1998-2016. *DFG-FOR816 Data Warehouse http://www.tropicalmountainforest.org/data_pre.do?citid=1860*.

Vergutz L, Manzoni S, Porporato A, Novais RF, Jackson RB. **2012**. Global resorption efficiencies and concentrations of carbon and nutrients in leaves of terrestrial plants. *Ecological Monographs* **82**: 205–220.

Wallis CIB, Homeier J, Peña J, Brandl R, Farwig N, Bendix J. **2019**. Modeling tropical montane forest biomass, productivity and canopy traits with multispectral remote sensing data. *Remote Sensing of Environment* **225**: 77–92.

Wang YP, Law RM, Pak B. **2010**. A global model of carbon, nitrogen and phosphorus cycles for the terrestrial biosphere. *Biogeosciences* **7**: 2261–2282.

White MA, Thornton PE, Running SW, Nemani RR. **2000**. Parameterization and Sensitivit y Analysis of the BIOME–BGC. *Earth interactions* **4**: 1–85.

Wilcke W, Leimer S, Peters T, Emck P, Rollenbeck R, Trachte K, Valarezo C, Bendix J. **2013**. The nitrogen cycle of tropical montane forest in Ecuador turns inorganic under environmental change. *Global Biogeochemical Cycles* **27**: 1194–1204.

Wilcke W, Velescu A, Leimer S, Bigalke M, Boy J, Valarezo C. **2019**. Temporal Trends of Phosphorus Cycling in a Tropical Montane Forest in Ecuador During 14 Years. *Journal of Geophysical Research: Biogeosciences* **124**: 1–17.

Wolf K, Veldkamp E, Homeier J, Martinson GO. **2011**. Nitrogen availability links forest productivity, soil nitrous oxide and nitric oxide fluxes of a tropical montane forest in southern Ecuador. *Global Biogeochemical Cycles* **25**: GB4009.

Wright IJ, Reich PB, Westoby M, Ackerly DD, Baruch Z, Bongers F, Cavender-Bares J, Chapin T, Cornellssen JHC, Diemer M, *et al.* 2004. The worldwide leaf economics spectrum. *Nature* **428**: 821–827.